CHAPTER 2.

Large-Scale Patterns of Insect and Disease Activity in the Conterminous United States, Alaska, and Hawaii from the National Insect and Disease Survey, 2018

Kevin M. Potter
Jeanine L. Paschke
Frank H. Koch
Erin M. Berryman

INTRODUCTION

Forest insects and diseases are having widespread ecological and economic impacts on the forests of the United States and may represent the most serious threats to the Nation's forests (Logan and others 2003, Lovett and others 2016, Tobin 2015). Insects and diseases cause changes in forest structure and function, species succession, and biodiversity, which may be considered negative or positive depending on management objectives (Edmonds and others 2011). Nearly all native tree species of the United States are affected by at least one injury-causing insect or disease agent, with exotic agents on average considerably more severe than native ones (Potter and others 2019a). Additionally, the genetic integrity of several native tree species is highly vulnerable to exotic diseases and insects (Potter and others 2019b).

An important task for forest managers, pathologists, and entomologists is recognizing and distinguishing between natural and excessive mortality, a task that relates to ecologically based or commodity-based management objectives (Teale and Castello 2011). The impacts of insects and diseases on forests vary from natural thinning to extraordinary levels of tree mortality, but insects and diseases are not necessarily enemies of the forest because they kill trees (Teale and Castello 2011). If disturbances, including insects and diseases, are viewed in their full ecological context, then some amount can be considered "healthy" to sustain the structure of the forest (Manion 2003, Zhang and others 2011) by causing tree mortality that culls weak competitors and releases resources that are needed to support the growth of surviving trees (Teale and Castello 2011).

Analyzing patterns of forest insect infestations, disease occurrences, forest declines, and related biotic stress factors is necessary to monitor the health of forested ecosystems and their potential impacts on forest structure, composition, biodiversity, and species distributions (Castello and others 1995). Introduced nonnative insects and diseases, in particular, can extensively damage the biodiversity, ecology, and economy of affected areas (Brockerhoff and others 2006, Mack and others 2000). Few forests remain unaffected by invasive species, and their devastating impacts in forests are undeniable, including, in some cases, wholesale changes to the structure and function of an ecosystem (Parry and Teale 2011).

Examining insect pest occurrences and related stress factors from a landscape-scale perspective is useful, given the regional extent of many infestations and the large-scale complexity of interactions between host distribution, stress factors, and the development of insect pest outbreaks (Holdenrieder and others 2004, Liebhold and others 2013). One such landscape-scale approach is detecting geographic patterns of disturbance, which allows for the identification of areas at greater risk of significant ecological and economic impacts and for the selection of locations for more intensive monitoring and analysis.

METHODS

Data

Forest Health Protection (FHP) national Insect and Disease Survey (IDS) data (FHP 2019) consist of information from low-altitude aerial survey and ground survey efforts by FHP and partners in State agencies. These data can be used to identify forest landscape-scale patterns associated with geographic hot spots of forest insect and disease activity in the conterminous 48 States and to summarize insect and disease activity by regions in the conterminous United States, Alaska, and Hawaii (Potter 2012, 2013; Potter and Koch 2012; Potter and Paschke 2013, 2014, 2015a, 2015b, 2016, 2017; Potter and others 2018, 2019).

The IDS data identify areas of mortality and defoliation caused by insect and disease activity, although some important forest insects (such as emerald ash borer [*Agrilus planipennis*] and hemlock woolly adelgid [*Adelges tsugae*]), diseases (such as laurel wilt [*Raffaelea lauricola*], Dutch elm disease [*Ophiostoma novo-ulmi*], white pine blister rust [*Cronartium ribicola*], and thousand cankers disease [*Geosmithia morbida*]), and mortality complexes (such as oak decline) are not easily detected or thoroughly quantified through aerial detection surveys. Such pests may attack hosts that are widely dispersed throughout forests with high tree species diversity or may cause mortality or defoliation that is otherwise difficult to detect. A pathogen or insect might be considered a mortality-causing agent in one location and a defoliation-causing agent in another, depending on the level of damage to the forest in a given area and the convergence of other stress factors such as drought. In some cases, the identified agents of mortality or defoliation are actually complexes of multiple agents summarized under an impact label related to a specific host tree species (e.g., "beech bark disease complex" or "yellow-cedar decline"). Additionally, differences in data collection, attribute recognition, and coding procedures among States and regions can complicate data analysis and interpretation of the results.

In 2018, IDS surveys of the conterminous United States covered about 211.34 million ha of both forested and unforested area (fig. 2.1), of which approximately 147.27 million ha encompassed areas with tree canopy cover (about 46.6 percent of the total 315.99-million-ha tree canopy area of the conterminous States). Nearly the entirety of this area was surveyed using the Digital Mobile Sketch Mapping (DMSM) approach, which is replacing the legacy Digital Aerial Sketch Mapping (DASM) approach (Berryman and McMahan 2019). In Alaska, roughly 13.65 million ha were surveyed in 2018, of which 9.9 million ha were forest or shrubland, about 12.7 percent of the total forest and shrubland area of the State. For Hawaii, about 933 000 ha were surveyed in 2018, with 598 000 of those in areas with tree canopy cover, approximately 69.4 percent of the State's total tree canopy area.

Digital Mobile Sketch Mapping includes tablet hardware, software, and data support processes that allow trained aerial surveyors

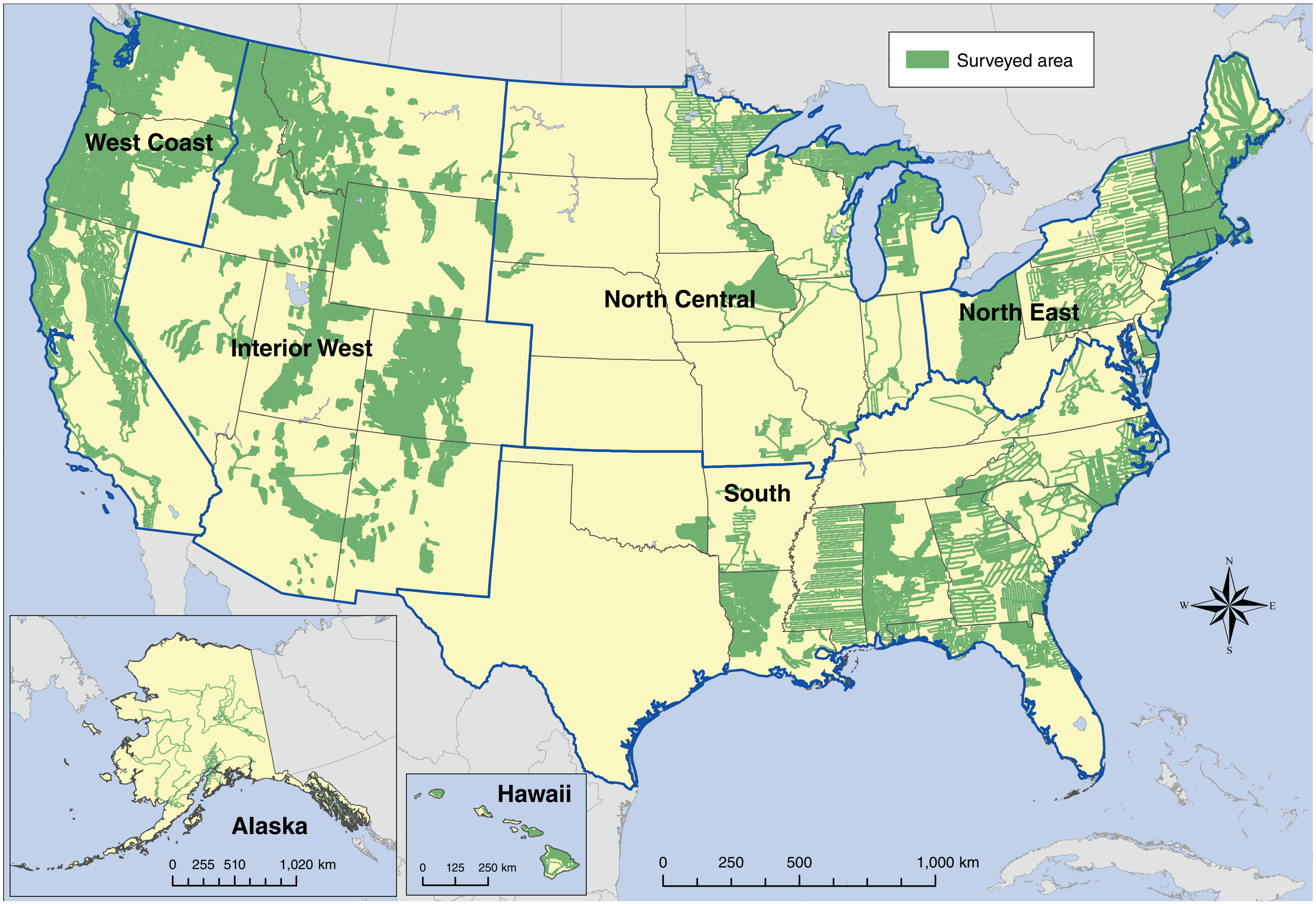

Figure 2.1—The extent of surveys for insect and disease activity conducted in the conterminous United States and Alaska in 2018. The blue lines delineate Forest Health Monitoring regions. Note: Alaska and Hawaii are not shown to scale with map of the conterminous United States. (Data source: U.S. Department of Agriculture Forest Service, Forest Health Protection)

in light aircraft, as well as ground observers, to record forest disturbances and their causal agents. Digital Mobile Sketch Mapping enhances the quality and quantity of forest health data while having the potential to improve safety by integrating with programs such as operational remote sensing (ORS), which uses satellite imagery to monitor disturbances in areas of higher aviation risk (FHP 2016). Geospatial data collected with DMSM are stored in the national IDS database. Digital Mobile Sketch Mapping includes both polygon geometry, used for damage areas where boundaries are discrete and obvious from the air, and point geometry, used for small clusters of damage where the size and shape of the damage are less important than recording the location of damage, such as for sudden oak death (caused by the pathogen *Phytophthora ramorum*), southern pine beetle (*Dendroctonus frontalis*), and some types of bark beetle damage in the West. For the 2018 data, these points were assigned an area of 0.8 ha (about 2 acres). Additionally, DMSM allows for the use of grid cells (240-, 480-, 960-, or 1920-m resolution) to estimate the percent of trees affected by damages that may be widespread and diffuse, such as those associated with European gypsy moth (*Lymantria dispar dispar*) and emerald ash borer. When calculating the total areas affected by each damage agent, we used the entire areas of these grid cells (e.g., 240-m cell = 5.76 ha).

Analyses

To estimate the extent of damaging insect and disease agents in 2018, we conducted two types of analyses. In the first, we reported the most widely detected mortality and defoliation agents in a series of tables. Specifically, the 2018 mortality and defoliation polygons were used to identify the select mortality and defoliation agents and complexes causing damage on >5000 ha of forest in the conterminous United States in that year. Similarly, we listed the five most widely reported mortality and defoliation agents and complexes within each of five Forest Health Monitoring (FHM) regions within the conterminous United States (West Coast, Interior West, North Central, North East, and South), as well as for Alaska and Hawaii where data were available.

Because of the insect and disease aerial sketch-mapping process (i.e., digitization of polygons by a human interpreter aboard the aircraft), all quantities are approximate "footprint" areas for each agent or complex, delineating areas of visible damage within which the agent or complex is present. Unaffected trees may exist within the footprint, and the amount of damage within the footprint is not reflected in the estimates of forest area affected. The sum of areas affected by all agents and complexes is not equal to the total affected area as a result of reporting multiple agents per polygon in some situations.

In our second set of analyses, we used the IDS data for 2018 to more directly estimate the impacts of insect- and disease-related mortality and defoliation on U.S. forests. These results are reported in a set of figures describing (1) the percent of surveyed tree canopy cover

area with insect- and disease-related mortality or defoliation within ecoregions across the United States and (2) geographic hot spots of insect- and disease-related mortality or defoliation across the conterminous 48 States and within the five FHM regions.

As an indicator of the extent of damaging insect and disease agents, we summarized the percent of surveyed tree canopy cover area experiencing mortality or defoliation for ecoregions within the conterminous 48 States and Hawaii, and for surveyed forest and shrubland in Alaska ecoregions. This is a change from previous FHM reports, in which we reported on the percent of regions *exposed to* mortality and defoliating agents based only on the footprint of mortality or defoliation polygon boundaries (masked by forest cover) because information on the percent of damage within polygons was not yet completely available. The new DMSM approach, however, allows surveyors to both define the extent of an area experiencing damage and to estimate a percent range of the area within the polygon that is affected (specifically 1–3 percent, 4–10 percent, 11–29 percent, 30–50 percent, and >50 percent). By multiplying the area of damage within each polygon (after masking by tree canopy cover) by the midpoint of the estimated range of percent affected, it is possible to generate an adjusted estimate of the area affected by each mortality or defoliation agent detection (Berryman and McMahan 2019). These individual estimates can be summed for all the polygons (intersected and dissolved) within an ecoregion and divided by the total surveyed tree canopy cover area within the ecoregion to generate an estimate of the percent of its canopy cover area affected by defoliating or mortality-causing agents. (Digital Mobile Sketch Mapping point data are also included in this estimate. Surveyors have the option to estimate the number of trees affected at a point and are required to assign an area value associated with each point [e.g., 1 acre {0.405 ha}], which is assumed to be 100 percent affected by its mortality or defoliation agent. These areas for all the points in an ecoregion are then added to the polygon-adjusted affected area estimates for the ecoregion.)

For the conterminous States, percent of surveyed tree canopy area with mortality or defoliation was calculated within each of 190 ecoregion sections (Cleland and others 2007). Similarly, the mortality and defoliation data were summarized for each of the 32 ecoregion sections in Alaska (Spencer and others 2002). In Hawaii, the percent of surveyed tree canopy area affected by mortality agents was calculated by ecoregions on each of the major islands of the archipelago (see ch. 1 for a description of these ecoregions). Statistics were not calculated for analysis regions in the conterminous United States or Hawaii with <5 percent of the tree canopy cover area surveyed, nor in Alaska with <2.5 percent of the forest and shrubland area surveyed.

The tree canopy data used for the conterminous States and Hawaii were resampled to 240 m from a 30-m raster dataset that

estimates percent tree canopy cover (from 0 to 100 percent) for each grid cell; this dataset was generated from the 2011 National Land Cover Database (NLCD) (Homer and others 2015) through a cooperative project between the Multi-Resolution Land Characteristics Consortium and the U.S. Department of Agriculture Forest Service, Geospatial Technology and Applications Center (GTAC) (Coulston and others 2012). For our purposes, we treated any cell with >0 percent tree canopy cover as forest. Comparable tree canopy cover data were not available for Alaska, so we instead created a 240-m-resolution layer of forest and shrub cover from the 2011 NLCD. (This is a change from previous Forest Health Monitoring national reports, for which the mortality and defoliation polygons were masked using a forest cover map [1-km resolution] derived from Moderate Resolution Imaging Spectroradiometer [MODIS] imagery by the Forest Service GTAC [USDA Forest Service 2008].)

Additionally, we used the Spatial Association of Scalable Hexagons (SASH) analytical approach to identify statistically significant geographic hot spots of mortality or defoliation in the conterminous 48 States. This method identifies locations where ecological phenomena occur at greater or lower frequency than expected by random chance and is based on a sampling frame optimized for spatial neighborhood analysis, adjustable to the appropriate spatial resolution, and applicable to multiple data types (Potter and others 2016). Specifically, it consists of dividing an analysis area into scalable equal-area hexagonal cells within which data are aggregated, followed by identifying statistically significant geographic clusters of hexagonal cells within which mean values are greater or less than those expected by chance. To identify these clusters, we employed a Getis-Ord (G_i*) hot spot analysis (Getis and Ord 1992) in ArcMap® 10.3 (ESRI 2015). We conducted two sets of hot spot analyses for both mortality-causing and defoliation-causing agents: one for the conterminous 48 States in their entirety, and one for each of the five FHM regions within the conterminous States. The low density of survey data in 2018 from Alaska and the small spatial extent of Hawaii (fig. 2.1) precluded the use of Getis-Ord G_i* hot spot analyses for these States.

The units of analysis were 9,810 hexagonal cells, each approximately 834 km^2 in area, generated in a lattice across the conterminous United States using intensification of the Environmental Monitoring and Assessment Program (EMAP) North American hexagon coordinates (White and others 1992). These coordinates are the foundation of a sampling frame in which a hexagonal lattice was projected onto the conterminous United States by centering a large base hexagon over the region (Reams and others 2005, White and others 1992). This base hexagon can be subdivided into many smaller hexagons, depending on sampling needs, and serves as the basis of the plot sampling frame for the Forest Inventory and Analysis (FIA) program (Reams and others 2005). Importantly, the hexagons maintain equal areas across the study region regardless of the degree of intensification of the EMAP

hexagon coordinates. In addition, the hexagons are compact and uniform in their distance to the centroids of neighboring hexagons, meaning that a hexagonal lattice has a higher degree of isotropy (uniformity in all directions) than does a square grid (Shima and others 2010). These are convenient and highly useful attributes for spatial neighborhood analyses. These scalable hexagons also are independent of geopolitical and ecological boundaries, avoiding the possibility of different sample units (such as counties, States, or watersheds) encompassing vastly different areas (Potter and others 2016). We selected hexagons 834 km^2 in area because this is a manageable size for making monitoring and management decisions in analyses that are national in extent (Potter and others 2016).

The Getis-Ord G_i* statistic was then used to identify clusters of hexagonal cells in which the percent of surveyed tree canopy area with mortality or defoliation was higher than expected by chance. This statistic allows for the decomposition of a global measure of spatial association into its contributing factors, by location, and is therefore particularly suitable for detecting instances of nonstationarity in a dataset, such as when spatial clustering is concentrated in one subregion of the data (Anselin 1992). Hexagons were excluded if they contained <5 percent tree canopy cover or if <1 percent of the tree canopy cover was surveyed in 2018.

The Getis-Ord G_i* statistic for each hexagon summed the differences between the mean values in a local sample, determined by a moving window consisting of the hexagon and its 18 first- and second-order neighbors (the 6 adjacent hexagons and the 12 additional hexagons contiguous to those 6) and a global mean. Our first analysis encompassed a global mean of all the forested hexagonal cells in the conterminous 48 States, while we conducted another set of analyses separately within each of the five FHM regions. The G_i* statistic was standardized as a *z*-score with a mean of 0 and a standard deviation of 1, with values >1.96 representing significant (p <0.025) local clustering of high values and values <-1.96 representing significant clustering of low values (p <0.025), since 95 percent of the observations under a normal distribution should be within approximately two (exactly 1.96) standard deviations of the mean (Laffan 2006). In other words, a G_i* value of 1.96 indicates that the local mean of the percentage of forest exposed to mortality-causing or defoliation-causing agents for a hexagon and its 18 neighbors is approximately two standard deviations greater than the mean expected in the absence of spatial clustering, while a G_i* value of -1.96 indicates that the local mortality or defoliation mean for a hexagon and its 18 neighbors is approximately two standard deviations less than the mean expected in the absence of spatial clustering. Values between -1.96 and 1.96 have no statistically significant concentration of high or low values. In other words, when a hexagon has a G_i* value between -1.96 and 1.96, mortality or defoliation damage within it and its 18 neighbors is not statistically different from a normal

expectation. As described in Laffan (2006), it is calculated as:

$$G_i^*(\boldsymbol{d}) = \frac{\sum_j w_{ij}(d)\, x_j - W_i^* \bar{x}^*}{s^* \sqrt{\frac{(n s_{1i}^*) - W_i^{*2}}{n-1}}}$$

where

G_i^* = the local clustering statistic (in this case, for the target hexagon)

i = the center of local neighborhood (the target hexagon)

d = the width of local sample window (the target hexagon and its first- and second-order neighbors)

x_j = the value of neighbor j

w_{ij} = the weight of neighbor j from location i (all the neighboring hexagons in the moving window were given an equal weight of 1)

n = number of samples in the dataset (the 4,303 hexagons containing >5 percent tree cover and with at least 1 percent of the canopy cover surveyed)

W_i^* = the sum of the weights

s^*_{1i} = the number of samples within d of the central location (19: the focal hexagon and its 18 first- and second-order neighbors)

$\bar{x}^*$ = mean of whole dataset (in this case, the 4,303 hexagons)

s^* = the standard deviation of whole dataset (for the 4,303 hexagons)

It is worth noting that the -1.96 and 1.96 threshold values are not exact because the correlation of spatial data violates the assumption of independence required for statistical significance (Laffan 2006). The Getis-Ord approach does not require that the input data be normally distributed because the local G_i^* values are computed under a randomization assumption, with G_i^* equating to a standardized *z*-score that asymptotically tends to a normal distribution (Anselin 1992). The *z*-scores are reliable, even with skewed data, as long as the distance band used to define the local sample around the target observation is large enough to include several neighbors for each feature (ESRI 2015).

RESULTS AND DISCUSSION

Conterminous United States Mortality

The national IDS survey data identified 56 different mortality-causing agents and complexes on approximately 2.13 million ha across the conterminous United States in 2018, slightly less than the combined land area of New Jersey and Rhode Island. By way of comparison, forests are estimated to cover approximately 252 million ha of the conterminous 48 States (Smith and others 2009). Twenty-two of the agents were detected on >5000 ha.

Fir engraver (*Scolytus ventralis*) was the most widespread mortality agent in 2018, detected on approximately 786 000 ha (table 2.1), or about 37 percent of the total mortality area, followed by emerald ash borer, which was identified on about 338 000 ha. Four other mortality agents

Table 2.1—Mortality agents and complexes affecting >5000 ha in the conterminous United States during 2018

Agents/complexes causing mortality, 2018	Area
	ha
Fir engraver	785 581
Emerald ash borer	337 618
Spruce beetle	143 342
Unknown bark beetle[a]	134 310
Mountain pine beetle	124 236
Western pine beetle	115,689
Eastern larch beetle	73 671
Douglas-fir beetle	56 390
Balsam woolly adelgid	48 072
Unknown	46 492
Sudden oak death	42 771
Jeffrey pine beetle	40 109
Flatheaded fir borer	31 088
Oak decline	24 260
Root disease and beetle complex	23 585
Twolined chestnut borer	22 689
Gypsy moth	22 187
Beech bark disease complex	16 629
Western balsam bark beetle	16 386
Pinyon ips	10 932
Southern pine beetle	9572
Ips engraver beetles	5689
Other (34)	21 802
Total, all mortality agents	**2 126 526**

Note: All values are "footprint" areas for each agent or complex. The sum of the individual agents is not equal to the total for all agents due to the reporting of multiple agents per polygon.

[a] In the Interior West, this is primarily damage on ponderosa pines. The group of bark beetles is known and varied, but not distinguishable from the air. Regions have characterized it as "Southwest bark beetle complex" consisting mainly of damage caused by roundheaded pine beetle, western pine beetle, and ips beetles.

and complexes were detected on >100 000 ha: spruce beetle (*D. rufipennis*) on 143 000 ha, unknown bark beetle on 134 000 ha (mostly damage on ponderosa pines [*Pinus ponderosa*] in the Interior West by a list of different bark beetles that are not possible to distinguish from the air), mountain pine beetle (*D. ponderosae*) on 124 000 ha, and western pine beetle (*D. brevicomis*) on 116 000 ha. Mortality from the western bark beetle group, which encompasses 16 different agents in the IDS data (table 2.2), was detected on approximately 1.43 million ha in 2018, representing about two-thirds of the total area on which mortality was recorded across the conterminous States.

The FHM West Coast region had the largest area on which mortality agents and complexes were detected, about 1.08 million ha (table 2.3). Approximately two-thirds of this area (721 000 ha) was exposed to fir engraver mortality. Twenty-two other mortality-causing agents and complexes were recorded, with the most widespread being western pine beetle (10.3 percent of the mortality area), mountain pine beetle (8.0 percent), sudden oak death (3.9 percent), and Jeffrey pine beetle (*D. jeffreyi*, 3.7 percent).

When estimating the amount of mortality occurring within the footprint of mortality in the West Coast region, we found that mortality was detected on 1.98 percent of the surveyed tree canopy area in the M261E–Sierra Nevada ecoregion section in California (fig. 2.2) as a result of infestation by fir engraver in red fir

Table 2.2—Beetle taxa included in the "western bark beetle" group

Western bark beetle mortality agents	
Common name	Scientific name
Cedar and cypress bark beetles	*Phloeosinus* spp.
Douglas-fir beetle	*Dendroctonus pseudotsugae*
Douglas-fir engraver	*Scolytus unispinosus*
Fir engraver	*Scolytus ventralis*
Ips engraver beetles	*Ips* spp.
Jeffrey pine beetle	*Dendroctonus jeffreyi*
Mountain pine beetle	*Dendroctonus ponderosae*
Pine engraver	*Ips pini*
Pinyon ips	*Ips confuses*
Root disease and beetle complex	N/A
Roundheaded pine beetle	*Dendroctonus adjunctus*
Silver fir beetle	*Pseudohylesinus sericeus*
Spruce beetle	*Dendroctonus rufipennis*
Unknown bark beetle	N/A
Western balsam bark beetle	*Dryocoetes confuses*
Western pine beetle	*Dendroctonus brevicomis*

(*Abies magnifica*) and white fir (*A. concolor*), and to a lesser degree by Jeffrey pine beetle, mountain pine beetle, and western pine beetle in pine species. The same agents resulted in 0.86 and 0.78 percent of surveyed canopy cover mortality in two ecoregion sections immediately north of the Sierra Nevada, M261D–Southern Cascades and M261G–Modoc Plateau, respectively. In the hot spot analysis encompassing the entire conterminous United States, a geographic hot spot of high mortality was detected in M261E–Sierra Nevada, while hot spots of moderate mortality were identified in neighboring ecoregions, including M261D–Southern Cascades and M261G–Modoc Plateau (fig. 2.3A). Similar hot spots were identified in the analysis limited to the West Coast FHM region (fig. 2.3B).

Elsewhere in the West Coast region, the M332G–Blue Mountains ecoregion section of northeastern Oregon had mortality on 0.66 percent of the surveyed tree canopy cover, as a result of fir engraver, western pine beetle, mountain pine beetle, and Douglas-fir beetle (*D. pseudotsugae*). Moderate-mortality hot spots were identified in this ecoregion section, both in the analyses of the conterminous States and of the West Coast FHM region.

Sudden oak death in tanoak (*Notholithocarpus densiflorus*), as well as some flatheaded fir borer (*Phaenops drummondi*) in Douglas-fir, resulted in 0.65 percent mortality of surveyed canopy area in 263A–Northern California Coast. Sudden oak death, along with a suite of bark beetles, was also an important mortality agent in 261A–Central California Coast (0.43 percent mortality) and M261B–Northern California Coast Ranges (0.40 percent mortality). A moderate-mortality hot spot associated with sudden oak death was detected in these ecoregion sections. Meanwhile, mountain pine beetle in lodgepole pine (*P. contorta*) was the primary factor in the respective 0.46 and 0.29 percent mortality in the surveyed canopy areas of M333A–Okanogan Highland and M242D–Northern Cascades in northern Washington. A variety of pine beetles, especially pinyon ips (*Ips confusus*) in singleleaf

Table 2.3—The top five mortality agents or complexes for each Forest Health Monitoring region, and for Alaska and Hawaii, in 2018

Mortality agents and complexes, 2018	Area
	ha
Interior West	
Spruce beetle	142 872
Unknown bark beetle[a]	133 036
Fir engraver	64 328
Balsam woolly adelgid	43 625
Douglas-fir beetle	37 791
Other mortality agents (19)	100 464
Total, all mortality agents and complexes	**517 183**
North Central	
Emerald ash borer	323 707
Eastern larch beetle	73 671
Oak decline	23 713
Beech bark disease complex	16 629
Unknown	1528
Other mortality agents (10)	2181
Total, all mortality agents and complexes	**440 926**
North East	
Twolined chestnut borer	22 280
Gypsy moth	22 187
Emerald ash borer	11 271
Southern pine beetle	5214
Unknown	2409
Other mortality agents (16)	6969
Total, all mortality agents and complexes	**70 060**
South	
Southern pine beetle	4358
Ips engraver beetles	4163
Emerald ash borer	2639
Unknown	2062
Unknown bark beetle	166
Other mortality agents (1)	<1
Total, all mortality agents and complexes	**13 365**

Mortality agents and complexes, 2018	Area
	ha
West Coast	
Fir engraver	721 252
Western pine beetle	111 946
Mountain pine beetle	86 702
Sudden oak death	42 771
Jeffrey pine beetle	40 107
Other mortality agents (18)	103 057
Total, all mortality agents and complexes	**1 084 994**
Alaska	
Spruce beetle	239 799
Yellow-cedar decline	7171
Unknown canker	2287
Northern spruce engraver	661
Western balsam bark beetle	45
Other mortality agents (2)	16
Total, all mortality agents and complexes	**249 976**
Hawaii	
Unknown	46 054
Total, all mortality agents and complexes	**46 054**

Note: The total area affected by other agents is listed at the end of each section. All values are "footprint" areas for each agent or complex. The sum of the individual agents is not equal to the total for all agents due to the reporting of multiple agents per polygon.

[a] In the Interior West, this is primarily damage on ponderosa pines. The group of bark beetles is known and varied, but not distinguishable from the air. Regions have characterized it as "Southwest bark beetle complex" consisting mainly of damage caused by roundheaded pine beetle, western pine beetle, and ips beetles.

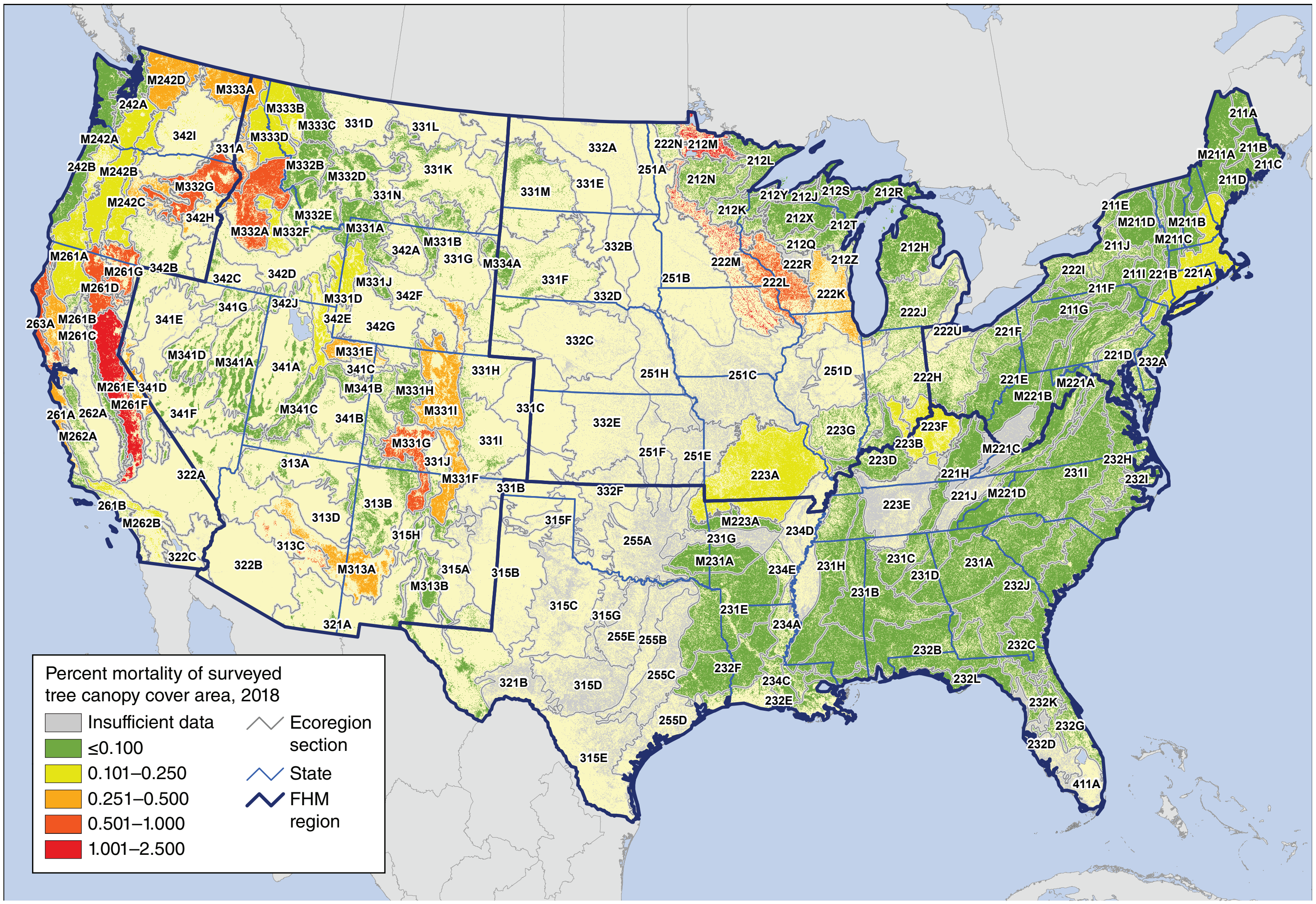

Figure 2.2—The percent of surveyed tree canopy cover area with insect and disease mortality, by ecoregion section within the conterminous 48 States, for 2018. The gray lines delineate ecoregion sections (Cleland and others 2007). The 240-m tree canopy cover is based on data from a cooperative project between the Multi-Resolution Land Characteristics Consortium (Coulston and others 2012) and the Forest Service Geospatial Technology and Applications Center using the 2011 National Land Cover Database. (Data source: U.S. Department of Agriculture Forest Service, Forest Health Protection)

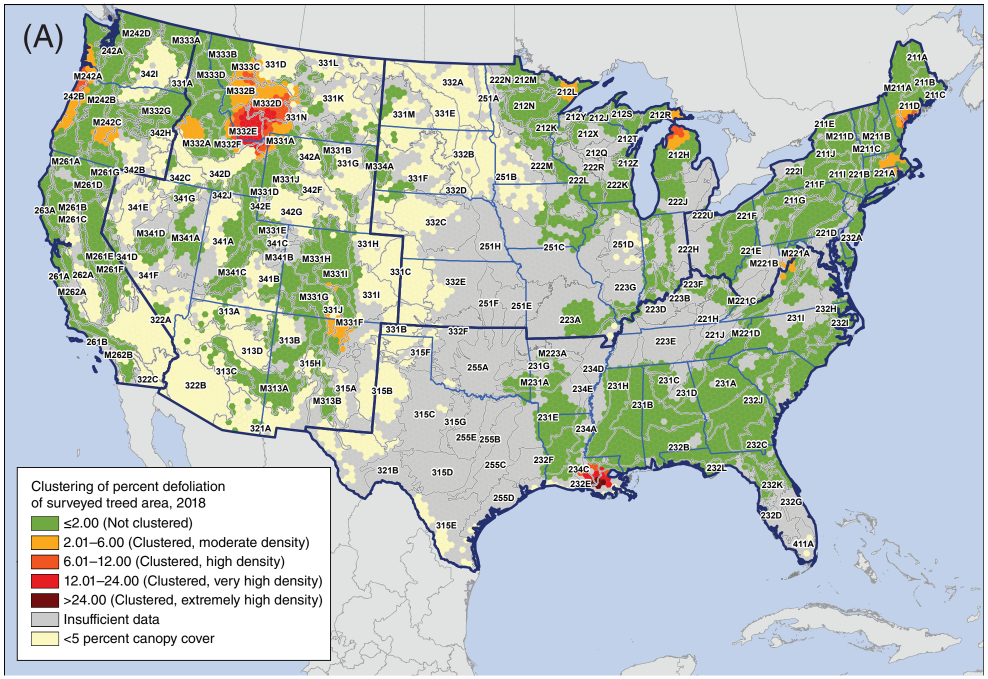

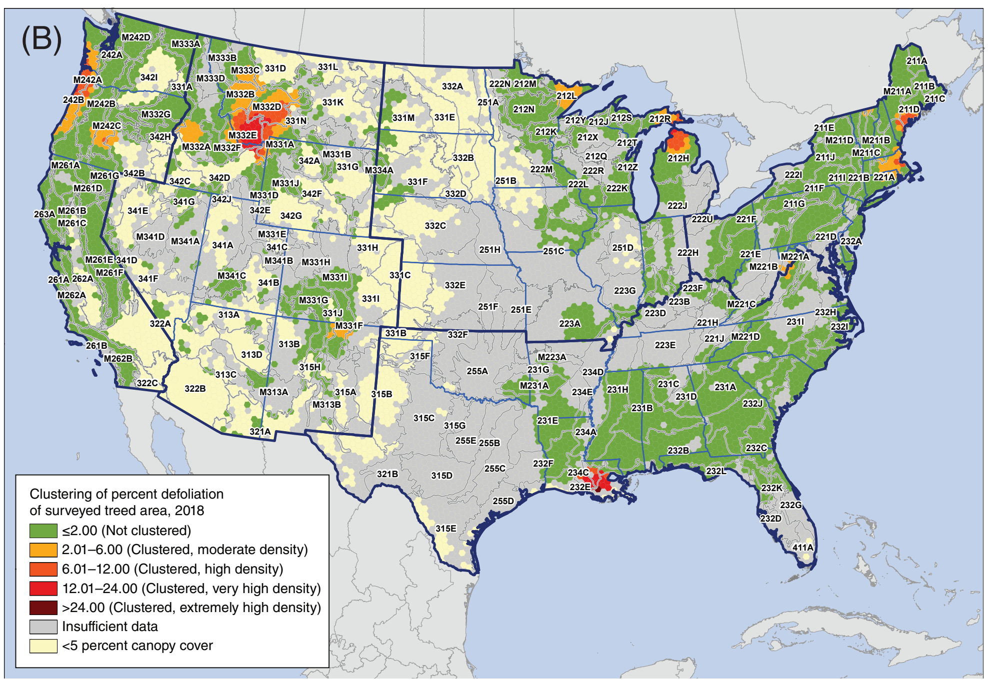

Figure 2.3—Hot spots of percent of surveyed tree canopy cover area with insect and disease mortality in 2018 for (A) the conterminous 48 States and (B) for separate Forest Health Monitoring regions, by hexagons containing >5 percent tree canopy cover. Values are Getis-Ord Gi scores, with values >2 representing significant clustering of high mortality occurrence densities and values <-2 representing significant clustering of low mortality occurrence densities. The gray lines delineate ecoregion sections (Cleland and others 2007), and blue lines delineate Forest Health Monitoring regions. Tree canopy cover is based on data from a cooperative project between the Multi-Resolution Land Characteristics Consortium (Coulston and others 2012) and the Forest Service Geospatial Technology and Applications Center using the 2011 National Land Cover Database. (Data source: U.S. Department of Agriculture Forest Service, Forest Health Protection)*

pinyon (*P. monophylla*), caused the 0.26 percent mortality of surveyed canopy area in 341D–Mono in east-central California.

Twenty-four mortality-causing agents and complexes were detected across 517 000 ha of the FHM Interior West region in 2018 (table 2.3). Of this mortality footprint, about 28 percent was attributed to spruce beetle (143 000 ha) and 26 percent to unknown bark beetles (133 000 ha). Other widespread mortality agents were fir engraver detected on 64 000 ha (12.4 percent), balsam woolly adelgid (*Adelges piceae*) on 44 000 ha (8.4 percent), and Douglas-fir beetle on 38 000 ha (7.3 percent) (table 2.3).

The estimate of the percent of mortality within the mortality footprint of the region, meanwhile, indicated that three ecoregion sections in the Interior West experienced 0.501 to 1 percent of mortality of surveyed tree canopy cover (fig. 2.2). In central Arizona, the 313C–Tonto Transition ecoregion section had 0.74 percent mortality, mostly caused by an unknown bark beetle infesting ponderosa pine. The M332A–Idaho Batholith ecoregion section in central Idaho experienced 0.52 percent mortality of surveyed tree cover as a result of spruce beetle mortality in Engelmann spruce (*Picea engelmannii*), mountain pine beetle mortality in lodgepole pine, Douglas-fir beetle mortality in Douglas-fir, and balsam woolly adelgid and root disease and beetle complex in subalpine fir (*Abies lasiocarpa*). Finally, the mortality detected in M331G–South-Central Highlands in southwestern Colorado and north-central New Mexico (>0.50 percent) was caused mostly by spruce beetle in Engelmann spruce and Douglas-fir beetle in Douglas-fir.

The conterminous States hot spot analysis revealed three moderate-mortality hot spots in the region: M332A–Idaho Batholith in central Idaho, M331G–South-Central Highlands in Colorado and New Mexico, and 313C–Tonto Transition in Arizona (fig. 2.3A). In the regional analysis, each of these was a high-mortality hot spot, with additional moderate hot spots found in Colorado (M331I–Northern Parks and Ranges; spruce beetle and western balsam bark beetle), Utah (M331E–Uinta Mountains and M331D–Overthrust Mountains; spruce beetle and root disease and beetle complex), and Arizona (322A–Mojave Desert; pinyon ips and unknown bark beetle) (fig. 2.3B).

In 2018, surveyors recorded approximately 441 000 ha with damage in the FHM North Central region, with approximately three-fourths of the mortality attributed to emerald ash borer (324 000 ha) (table 2.3). Of the other 14 mortality agents recorded, eastern larch beetle (*Dendroctonus simplex*) was the most widespread (16.7 percent of the mortality area), followed by oak decline (5.4 percent), and beech bark disease complex (3.8 percent).

The ecoregion section with the greatest mortality of surveyed tree canopy cover was 212M–Northern Minnesota and Ontario, where eastern larch beetle resulted in 2.05 percent mortality of surveyed tree canopy cover

(fig. 2.2). Emerald ash borer was the most important mortality agent in 222M–Minnesota and Northeast Iowa Morainal-Oak Savannah (1.39 percent mortality), 222L–North Central U.S. Driftless and Escarpment (0.73 percent mortality), and 222K–Southwestern Great Lakes Morainal (0.43 percent). Oak decline was relatively widely detected in south-central Indiana (223B–Interior Low Plateau-Transition Hills and 223D–Interior Low Plateau) and southern Missouri (223A–Ozark Highlands).

In the analysis of the conterminous States, three geographic hot spots of very high mortality associated with emerald ash borer were detected in 251C–Central Dissected Till Plains of southeastern Iowa; 222M–Minnesota and Northeast Iowa Morainal-Oak Savannah of northeastern Iowa; and 222L–North Central U.S. Driftless and Escarpment of southwestern Wisconsin, northeastern Iowa, and southeastern Minnesota (fig. 2.3A). A hot spot of high mortality, meanwhile, was associated with eastern larch beetle in 212M–Northern Minnesota and Ontario. The same hot spots were revealed in the analysis focusing on the North Central FHM region but were of lower intensity (fig. 2.3B).

In the North East FHM region, mortality in 2018 was recorded on approximately 70 000 ha, attributed to 21 mortality agents and complexes (table 2.3). Two agents, twolined chestnut borer (*Agrilus bilineatus*) and gypsy moth, accounted for a nearly identical amount of this mortality (approximately 31 percent each), while emerald ash borer was associated with 16.1 percent.

The only ecoregion in the North East FHM region with >0.1 percent mortality of its surveyed treed area (0.13 percent) was 221A–Lower New England, where twolined chestnut borer in red oak stands was detected in Rhode Island, emerald ash borer was found in Connecticut, and gypsy moth was identified in Connecticut and Massachusetts (fig. 2.2). No mortality hot spots were revealed in the region in the analysis encompassing the conterminous States (fig. 2.3A), but a hot spot in the regional analysis spanned Long Island Sound, including the gypsy moth and emerald ash borer mortality in Connecticut to the north and southern pine beetle mortality in pitch pine (*P. rigida*) on Long Island to the south (fig. 2.3B).

In the South FHM region, surveyors identified 13 000 ha of mortality from six agents (table 2.3). Southern pine beetle was the most commonly detected agent, on 4400 ha (32.6 percent), followed closely by ips engraver beetles (4200 ha, 31.6 percent). Emerald ash borer was found on an additional 2600 ha (19.7 percent).

No ecoregions in the South had mortality exceeding 0.1 percent as a result of mortality within the region (fig. 2.2). (Three ecoregions exceeded this threshold because of mortality in the neighboring North Central region.) No mortality hot spots were identified in the analysis of the conterminous States (fig. 2.3A), but several were detected in the regional hot spot analysis (fig. 2.3B). Three of these hot spots were associated with southern pine beetle, in south-central Mississippi (231B–Coastal Plains-Middle and 232B–Gulf Coastal Plains and Flatwoods);

southwestern Mississippi and eastern Louisiana (231H–Coastal Plains-Loess); and western North Carolina (M221D–Blue Ridge Mountains). A hot spot in central Arkansas (M231A–Ouachita Mountains and 231G–Arkansas Valley) was caused by ips engraver beetles, while another in northern Kentucky (223F–Interior Low Plateau-Bluegrass and 221E–Southern Unglaciated Allegheny Plateau) was the result of emerald ash borer infestation. Finally, the agent or agents causing a hot spot in northeastern North Carolina and southeastern Virginia (232I–Northern Atlantic Coastal Flatwoods) were reported as unknown by surveyors.

Conterminous United States Defoliation

In 2018, the national IDS survey identified 56 defoliation agents and complexes affecting approximately 1.72 million ha across the conterminous United States (table 2.4), an area similar to the land area of Connecticut and Delaware combined. The most widespread defoliation agent was western spruce budworm (*Choristoneura freemani*), detected on approximately 654 000 ha, or 38 percent of the total area with defoliation. Five other agents were also detected on >100 000 ha each: forest tent caterpillar (*Malacosoma disstria*) on 289 000 ha, Swiss needle cast on 199 000 ha, gyspy moth on 156 000 ha, and baldcypress leafroller (*Archips goyerana)* on 137 000 ha (table 2.4).

In 2018, the Interior West was the FHM region with the largest area on which defoliation agents were detected, with 20 defoliators identified on approximately 774 000 ha (table 2.5). Of this area, 84.2 percent

Table 2.4—Defoliation agents and complexes affecting >5000 ha in the conterminous United States in 2018

Agents/complexes causing defoliation, 2018	Area
	ha
Western spruce budworm	654 521
Forest tent caterpillar	289 136
Swiss needle cast	199 143
Gypsy moth	155 871
Baldcypress leafroller	136 741
Spruce budworm	90 474
Pandora moth	58 894
Browntail moth	55 130
Douglas-fir tussock moth	49 433
Unknown defoliator	46 203
White pine needle damage	19 267
Balsam woolly adelgid	14 613
Pinyon needle scale	10 835
Unknown	8417
Walkingstick	7857
Larch casebearer	7814
Spruce aphid	7355
Marssonina blight	7147
Scarlet oak sawfly	6843
Other (37)	24 167
Total, all defoliation agents	**1 722 675**

Note: All values are "footprint" areas for each agent or complex. The sum of the individual agents is not equal to the total for all agents due to the reporting of multiple agents per polygon.

Table 2.5—The top five defoliation agents or complexes for each Forest Health Monitoring region and for Alaska in 2018

Defoliation agents and complexes, 2018	Area
	ha
Interior West	
Western spruce budworm	651 491
Unknown defoliator	45 855
Douglas-fir tussock moth	44 883
Pinyon needle scale	10 824
Spruce aphid	7355
Other defoliation agents (15)	14 852
Total, all defoliation agents and complexes	**774 191**
North Central	
Forest tent caterpillar	119 128
Spruce budworm	90 474
Larch casebearer	6920
Unknown	4106
Gypsy moth	2671
Other defoliation agents (8)	3444
Total, all defoliation agents and complexes	**226 743**
North East	
Gypsy moth	143 361
Browntail moth	55 130
Forest tent caterpillar	32 805
White pine needle damage	19 267
Cherry scallop shell moth	2823
Other defoliation agents (11)	4565
Total, all defoliation agents and complexes	**257 861**

Defoliation agents and complexes, 2018	Area
	ha
South	
Forest tent caterpillar	136 802
Baldcypress leafroller	136 741
Gypsy moth	9839
Walkingstick	7857
Scarlet oak sawfly	6843
Other defoliation agents (2)	2241
Total, all defoliation agents and complexes	**170 680**
West Coast	
Swiss needle cast	199 143
Pandora moth	58 894
Balsam woolly adelgid	14 613
Douglas-fir tussock moth	4550
Larch needle cast	3932
Other defoliation agents (20)	8452
Total, all defoliation agents and complexes	**293 200**
Alaska	
Aspen leafminer	97 058
Birch leafminer	43 951
Unknown defoliator	25 590
Hemlock sawfly	19 655
Willow leaf blotchminer	14 473
Other defoliation agents (6)	4289
Total, all defoliation agents and complexes	**201 200**

Note: The total area affected by other agents is listed at the end of each section. All values are "footprint" areas for each agent or complex. The sum of the individual agents is not equal to the total for all agents due to the reporting of multiple agents per polygon.

was affected by western spruce budworm (651 000 ha). No other agent accounted for >6 percent of the total defoliated area in the region.

Ecoregion sections in the northern Rockies were particularly affected by western spruce budworm in 2018, with 7.1 percent of surveyed tree canopy area defoliated in M332E–Beaverhead Mountains in central Idaho and southwestern Montana, and with 3.9 percent of the M332D–Belt Mountains and 2.7 percent of the M332B–Northern Rockies and Bitterroot Valley, respectively, defoliated in western Montana (fig. 2.4). This outbreak in stands of subalpine fir and Douglas-fir was reflected in a hot spot of very high defoliation in the analyses both for the entire conterminous States (fig. 2.5A) and for the Interior West region (fig. 2.5B). Farther south, in south-central Colorado and northern New Mexico, western spruce budworm was the source of hot spots of moderate defoliation in M331F–Southern Parks and Rocky Mountain Range.

In west-central Idaho, meanwhile, Douglas-fir tussock moth (*Orgyia pseudotsugata*) was the source of a hot spot of moderate defoliation in M332A–Idaho Batholith (fig. 2.5), where 1.6 percent of surveyed tree canopy area was defoliated (fig. 2.4).

The West Coast FHM region recorded 25 defoliating agents on 293 000 ha (table 2.5). Swiss needle cast (caused by the fungus *Phaeocryptopus gaeumannii*) was the most widely reported, encompassing 68 percent of the total defoliated area (199 000 ha). Other widespread defoliation agents included pandora moth (*Coloradia pandora*) (59 000 ha, 20.1 percent) and balsam woolly adelgid (15 000 ha, 5.0 percent).

As a result of Swiss needle cast, a native disease that defoliates Douglas-fir, a hot spot of high defoliation was detected along the coast of Oregon and Washington (M242A–Oregon and Washington Coast Ranges) (fig. 2.5), an ecoregion section that experienced 3.6 percent defoliation of surveyed tree canopy area (fig. 2.4). An additional hot spot in central Oregon in the M242C–Eastern Cascades ecoregion section (of moderate defoliation in both the conterminous States and West Coast region analysis) was caused by an outbreak of pandora moth in ponderosa and lodgepole pine stands.

In the North East region, gypsy moth was the most widely identified defoliation agent among the 16 detected across 258 000 ha in 2018 (table 2.5). It was found on approximately 143 000 ha (55.6 percent of the total defoliated area), followed by browntail moth (*Euproctis chrysorrhoea*) on 55 000 ha (21.4 percent), forest tent caterpillar on 33 000 ha (12.7 percent), and white pine needle damage on 19 000 ha (7.5 percent).

The 211D–Central Maine Coastal Embayment ecoregion section had the highest defoliation of surveyed tree cover in the region (2.9 percent), as a result of browntail moth infestation of northern red oak (*Quercus rubra*) (fig. 2.4). Defoliation was 1.1 percent of surveyed canopy cover area, meanwhile, in neighboring 221A–Lower New England, where gypsy moth

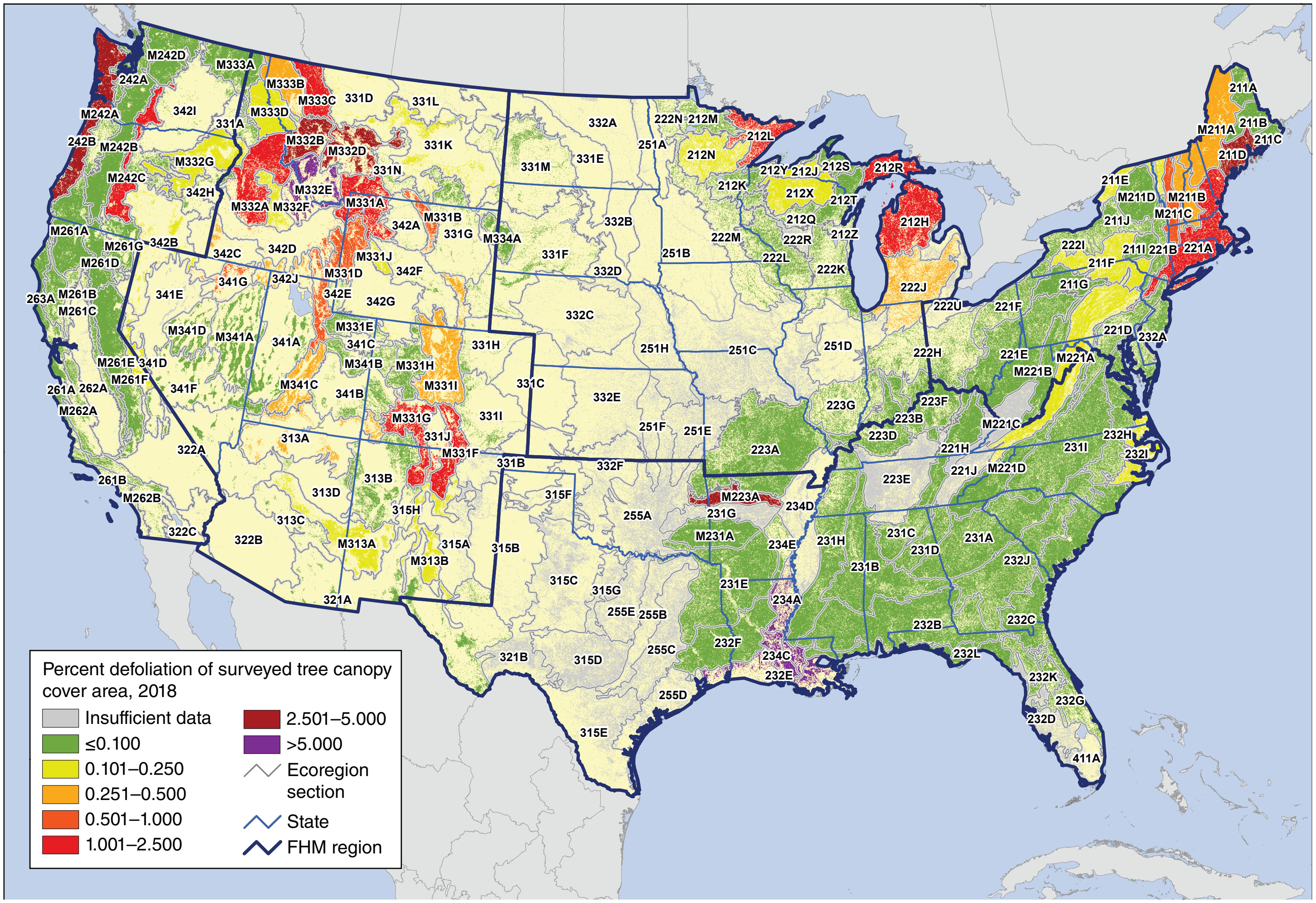

Figure 2.4—The percent of surveyed tree canopy cover area with insect and disease defoliation, by ecoregion section within the conterminous 48 States, for 2018. The gray lines delineate ecoregion sections (Cleland and others 2007). The 240-m tree canopy cover is based on data from a cooperative project between the Multi-Resolution Land Characteristics Consortium (Coulston and others 2012) and the Forest Service Geospatial Technology and Applications Center using the 2011 National Land Cover Database. (Data source: U.S. Department of Agriculture Forest Service, Forest Health Protection)

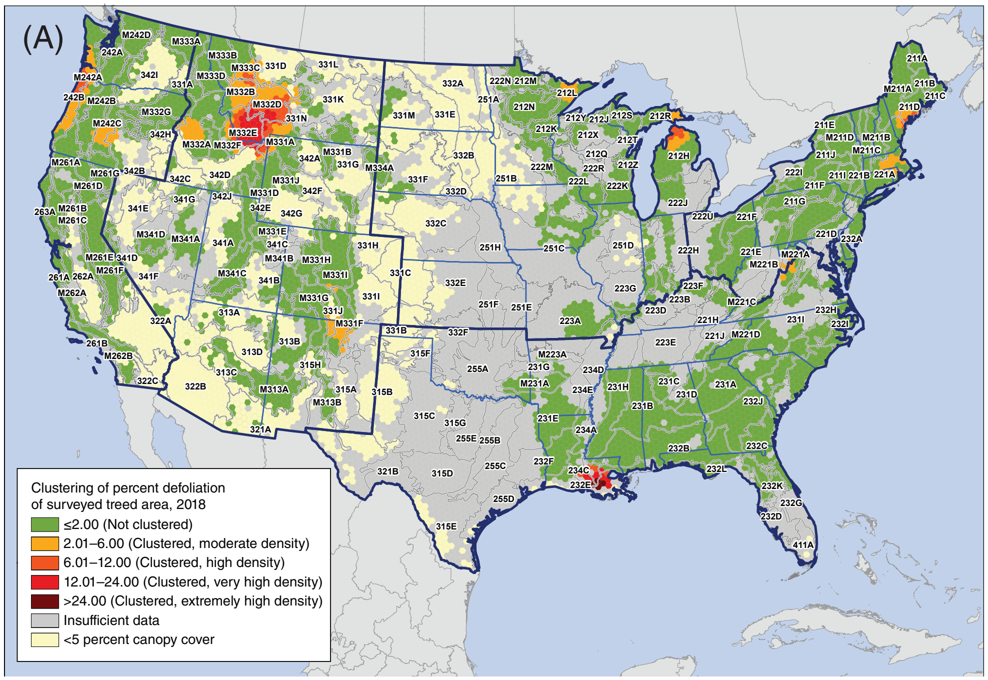

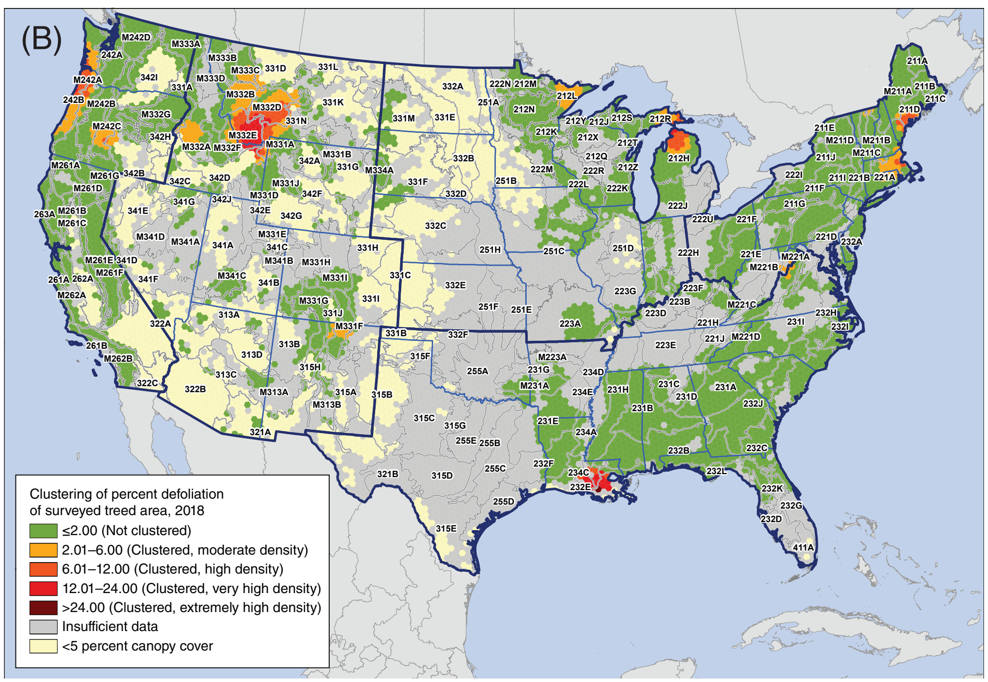

Figure 2.5—Hot spots of percent of surveyed tree canopy cover area with insect and disease defoliation in 2018 for (A) the conterminous 48 States and (B) for separate Forest Health Monitoring regions, by hexagons containing >5 percent tree canopy cover. Values are Getis-Ord Gi* *scores, with values >2 representing significant clustering of high defoliation occurrence densities. (No areas of significant clustering of low densities, <-2, were detected.) The gray lines delineate ecoregion sections (Cleland and others 2007), and blue lines delineate Forest Health Monitoring regions. Tree canopy cover is based on data from a cooperative project between the Multi-Resolution Land Characteristics Consortium (Coulston and others 2012) and the Forest Service Geospatial Technology and Applications Center using the 2011 National Land Cover Database. (Data source: U.S. Department of Agriculture Forest Service, Forest Health Protection)*

was widespread in hardwood stands. These two ecoregion sections were the locations of hot spots of high and moderate defoliation, respectively (fig. 2.5).

White pine needle damage in stands of eastern white pine (*P. strobus*) and forest tent caterpillar in hardwood forests in New England resulted in 0.6 percent defoliation of surveyed canopy area in M211C–Green-Taconic-Berkshire Mountains, 0.4 percent in M211A–White Mountains, and 0.3 percent in M211B–New England Piedmont (fig. 2.4). Additionally, gypsy moth activity resulted in a hot spot of moderate defoliation along the border of West Virginia and Virginia (fig. 2.5).

Thirteen agents and complexes, meanwhile, were associated with approximately 227 000 ha with defoliation in the North Central FHM region (table 2.5). Forest tent caterpillar and spruce budworm (*Choristoneura fumiferana*) were the most commonly detected defoliators, representing 52.5 percent and 39.9 percent of the total defoliation in the region (119 000 ha and 90 000 ha, respectively). Larch casebearer (*Coleophora laricella*) was also somewhat widespread (7000 ha, or 3.1 percent of the total area with defoliation).

A handful of ecoregion sections in the Great Lakes States exhibited the highest levels of defoliation (fig. 2.4):

- In northern Michigan, forest tent caterpillar caused 1.9 percent defoliation of surveyed canopy cover area in 212R–Eastern Upper Peninsula and 1.7 percent in 212H–Northern Lower Peninsula.
- In northeastern Minnesota, spruce budworm resulted in 1.6 percent defoliation in 212L–Northern Superior Uplands.
- In southern Michigan, gypsy moth was associated with defoliation on 0.3 percent of the surveyed tree canopy area in 222J–South Central Great Lakes.

The national (fig. 2.5A) and regional (fig. 2.5B) analyses revealed hot spots of high to very high defoliation in northern Michigan, and of moderate defoliation in northeastern Minnesota.

During 2018, surveyors documented about 171 000 ha with defoliation in the South (table 2.5), with both forest tent caterpillar and baldcypress leafroller (*Archips goyerana*) detected on about 137 000 ha, or 80 percent of the area with defoliation. (Both agents were reported together across large areas of southern Louisiana.) Gypsy moth was recorded on an additional 10 000 ha (5.8 percent).

The ecoregion sections nationally with the highest and third highest percent defoliation were in southern Louisiana: 234C–Atchafalaya and Red River Alluvial Plains (16.1 percent) and 232E–Louisiana Coastal Prairie and Marshes (7.1 percent) (fig. 2.4). Baldcypress leafroller and forest tent caterpillar were the major defoliation agents here and were the causes of the hot spots of extremely high defoliation in the same area, revealed by the analyses of both the entire conterminous United States and the South (fig. 2.5). Relatively high defoliation (3.3 percent)

was also found in M223A–Boston Mountains in northern Arkansas, as a result of an infestation of walkingstick (*Diapheromera femorata*) in hardwood forests there (fig. 2.4).

Alaska and Hawaii

In Alaska, seven mortality agents and complexes were detected on 250 000 ha in 2018 (table 2.3). As in recent years, spruce beetle was the most widely detected mortality agent, encompassing 95.9 percent of the total area with mortality (240 000 ha). A much smaller area of yellow-cedar (*Chamaecyparis nootkatensis*) decline was detected (7000 ha, 2.9 percent of the total). Surveyors attributed a further 2000 ha with mortality to an unknown canker on quaking aspen (*Populus tremuloides*).

An extensive outbreak of spruce beetle caused 133A–Cook Inlet Basin, in the south-central part of the State, to have the highest mortality of surveyed forest and shrubland (1.7 percent) (fig. 2.6). The spruce beetle infestation extended into the neighboring M243B–Alaska Peninsula and M133B–Alaska Range Extension ecoregion sections (0.4 percent mortality in each).

Also in 2018, Alaska surveyors identified 11 defoliators on 201 000 ha (table 2.5). Almost half of the area with defoliation (97 000 ha, 48.2 percent) was attributed to aspen leafminer (*Phyllocnistis populiella*). The next most commonly detected defoliation agent was birch leafminer (*Fenusa pusilla*) on 44 000 ha (21.8 percent). Almost 13 percent of the area with defoliation was associated with an unknown defoliator (26 000 ha), while 9.8 percent was caused by hemlock sawfly (*Neodiprion tsugae*, 20 000 ha) and 7.2 percent with willow leaf blotchminer (*Micrurapteryx salicifoliella*, 14 000 ha).

Defoliation was relatively high across much of Alaska in 2018, particularly the central part of the State. Defoliation was highest in 132C–Tanana-Kuskokwim Lowlands, slightly more than 2.5 percent of surveyed forest and shrubland (fig. 2.7), where aspen leafminer was prevalent. Damage from aspen leafminer was also commonly found in nearby M132C–Yukon-Tanana Uplands (1.2 percent defoliation) and 133B–Copper River Basin (slightly more than 1.0 percent). Willow leaf blotchminer was the most widespread defoliation agent, along with aspen leafminer, in 132A–Yukon-Old Crow Basin (1.9 percent defoliation). In 133A–Cook Inlet Basin (1.8 percent defoliation) of south-central Alaska, birch leafminer was the primary defoliator. In the southwestern part of the State, speckled green fruitworm (*Orthosia hibisci*) was the most commonly detected defoliation agent in M131B–Ahklun Mountains (just more than 1.0 percent defoliation).

In Hawaii, meanwhile, approximately 46 000 ha with mortality were delineated in 2018 (table 2.3). None of this mortality was assigned to an agent, but at least some of this was likely caused by rapid ʻōhiʻa death, a wilt disease that affects ʻōhiʻa lehua (*Metrosideros polymorpha*), a highly ecologically and culturally important tree in Hawaiian native forests (University of Hawaiʻi 2019). Rapid ʻōhiʻa death is caused by the fungal pathogens *Ceratocystis lukuohia* and

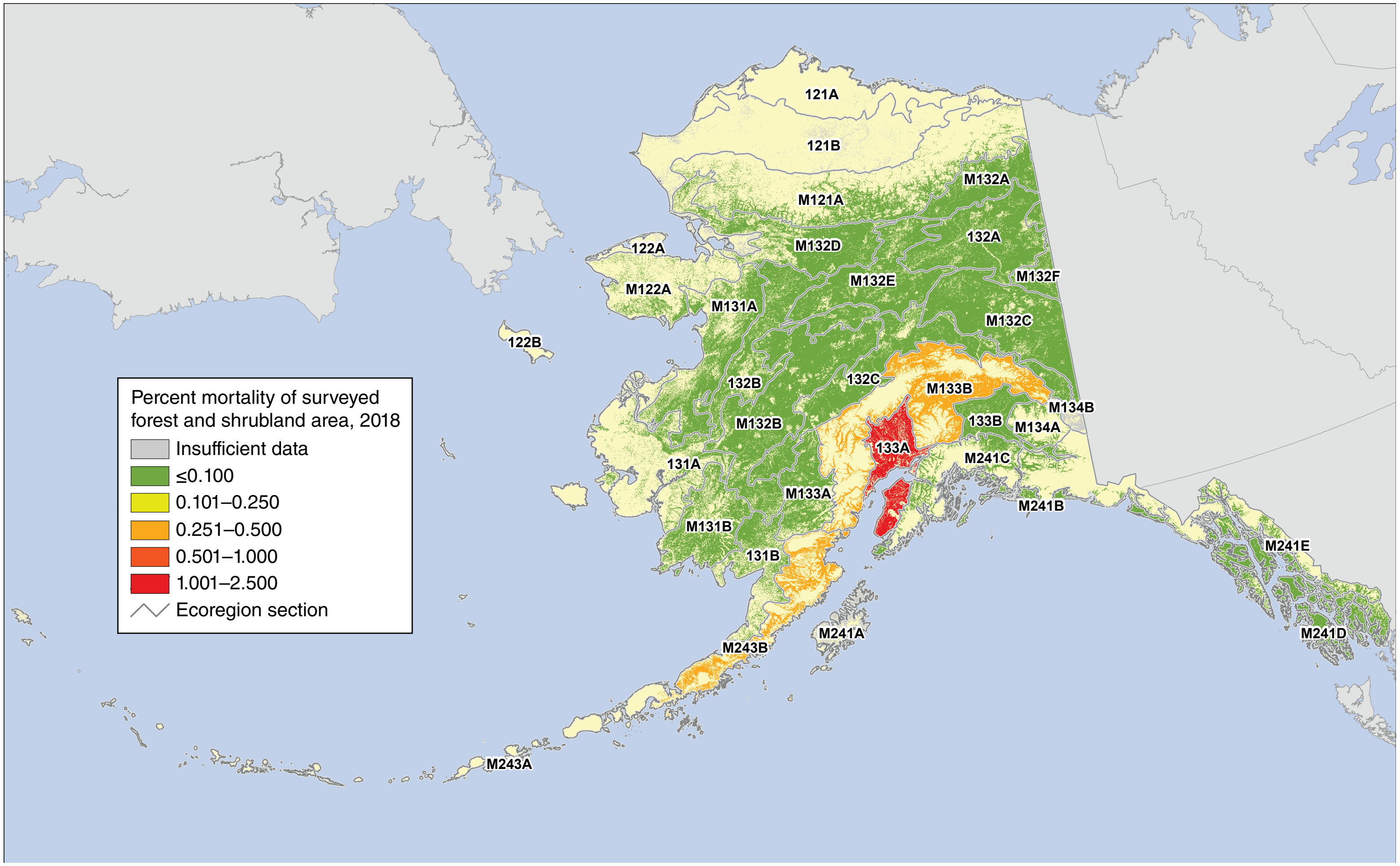

Figure 2.6—Percent of 2018 surveyed Alaska forest and shrubland area within ecoregions with mortality caused by insects and diseases. The gray lines delineate ecoregion sections (Spencer and others 2002). Forest and shrub cover is derived from the 2011 National Land Cover Database. (Data source: U.S. Department of Agriculture Forest Service, Forest Health Protection)

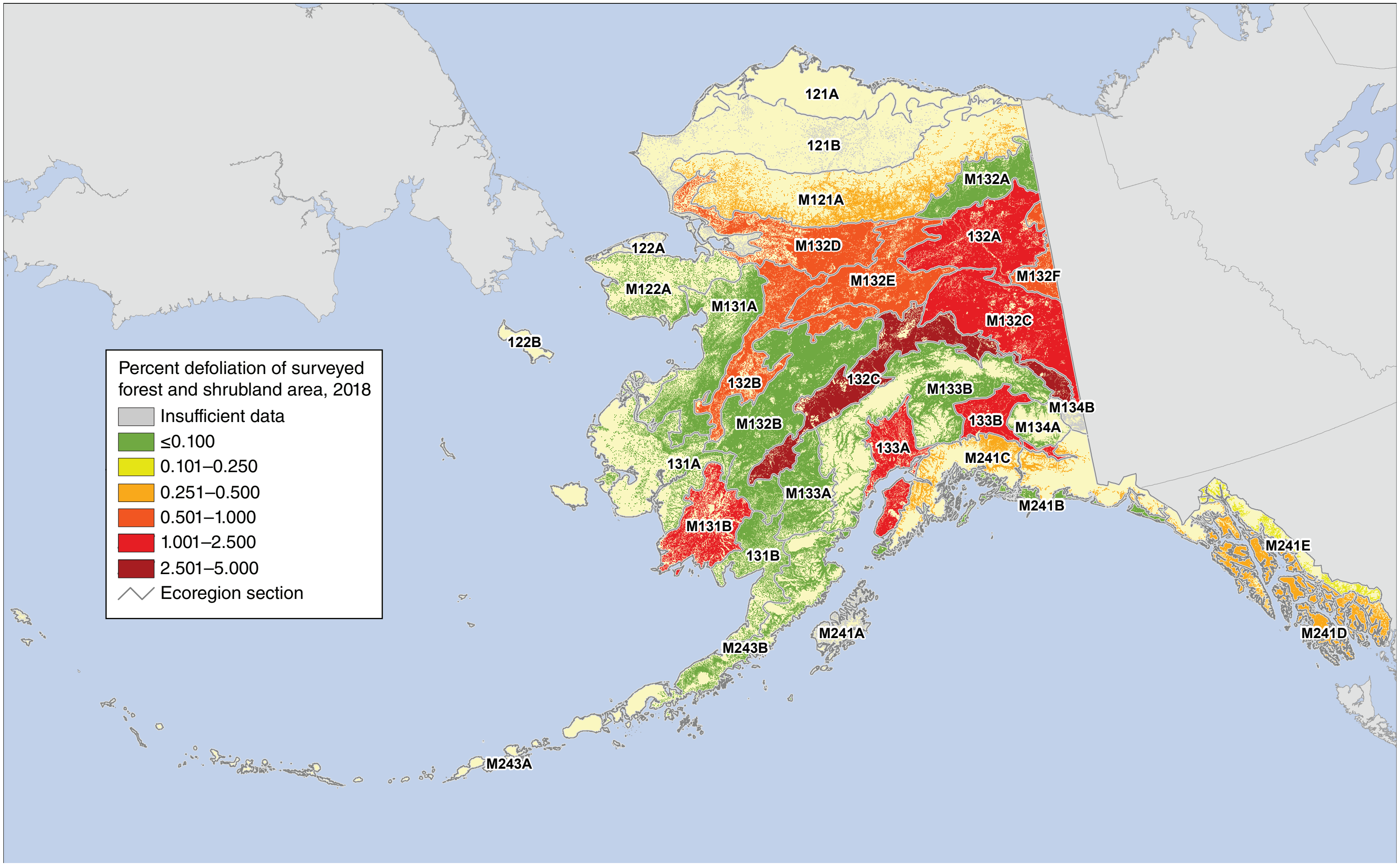

Figure 2.7—Percent of 2018 surveyed Alaska forest and shrubland area within ecoregions with defoliation caused by insects and diseases. The gray lines delineate ecoregion sections (Spencer and others 2002). Forest and shrub cover is derived from the 2011 National Land Cover Database. (Data source: U.S. Department of Agriculture Forest Service, Forest Health Protection)

C. huliohia, but *C. lukuohia* is more aggressive than *C. huliohia* (Barnes and others 2018). Both pathogens have been confirmed on the islands of Hawai‘i (the Big Island) and Kaua‘i, while individual trees infected with *C. huliohia* have been detected on Maui and O‘ahu (University of Hawai‘i 2019). Mortality detected in 2018 was high across many of the wetter areas of the Big Island, particularly in the Montane Wet-Hawai‘i-Kona (MWh-ko) ecoregion on the leeward (west) side of the island, where 2.35 percent of the surveyed tree canopy area had mortality (fig. 2.8). On the south side of the island, Montane Wet-Hawai‘i-Ka‘ū (MWh-ka) had 1.00 percent mortality of surveyed canopy area, while on the windward (east) side, Lowland Wet-Hawai‘i-Hilo-Puna (LWh-hp) had 0.90 percent and Montane Wet-Hawai‘i-Hilo-Puna (MWh-hp) had 0.45 percent. Meanwhile, upland wet areas of Maui also had relatively high mortality. Wet areas on Maui also experienced relatively high mortality, including Lowland Wet-Maui-West (LWm-w), where mortality was 1.13 percent of the surveyed tree canopy area; Montane Wet-Maui-East (MWm-e), 0.66 percent; Mesic-Maui-West (MEm-w), 0.63 percent; and Montane Wet-Maui-West (MWm-w), 0.47 percent. No defoliation was documented in Hawaii during 2018.

CONCLUSION

Continued monitoring of insect and disease outbreaks across the United States will be necessary for determining appropriate follow-up investigation and management activities. Due to the limitations of survey efforts to detect certain important forest insects and diseases, the pests and pathogens discussed in this chapter do not include all the biotic forest health threats that should be considered when making management decisions and budget allocations. However, large-scale assessments of mortality and defoliation severity, including geographical hot spot detection analyses, offer a useful approach for identifying geographic areas where the concentration of monitoring and management activities might be most effective.

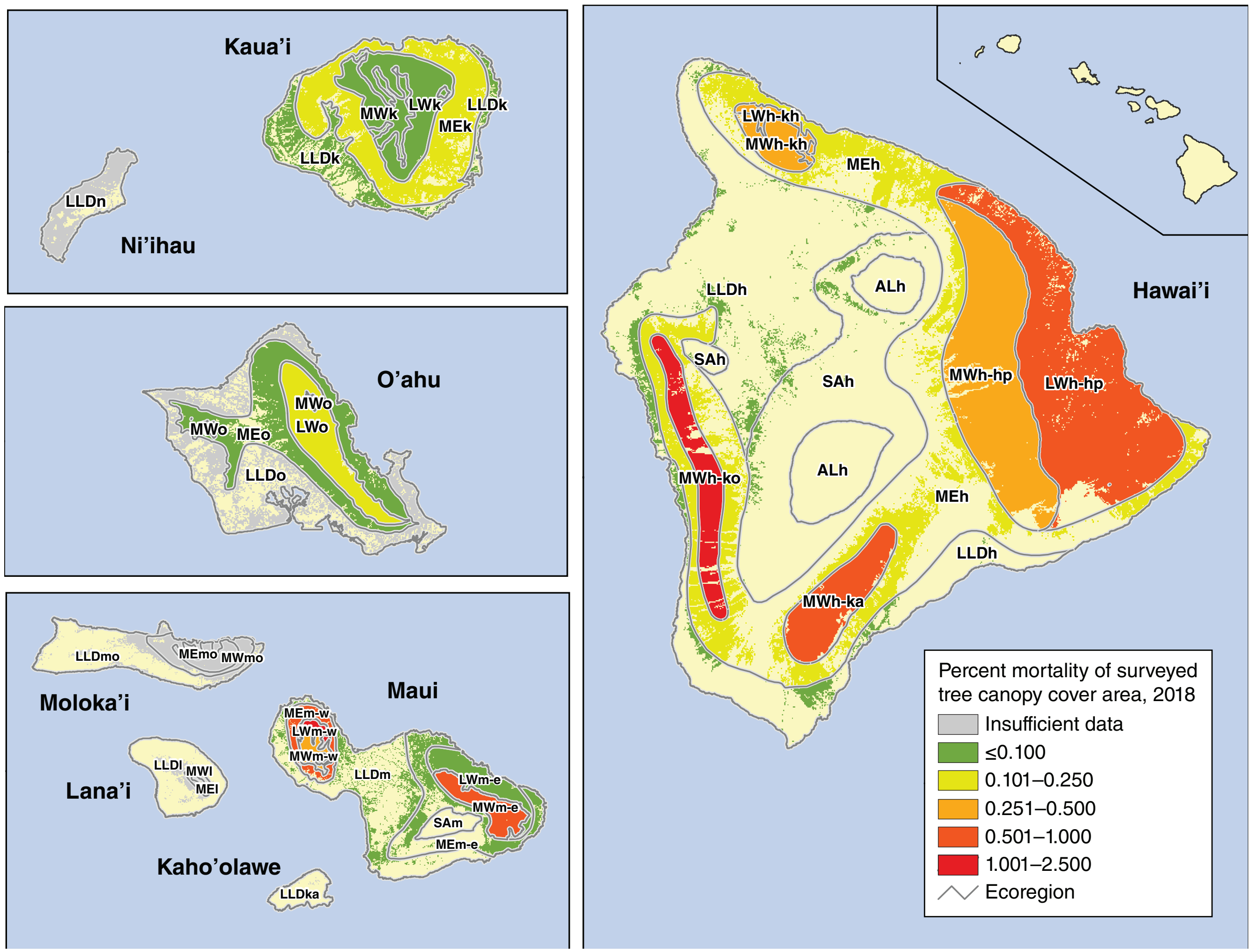

Figure 2.8—Percent of 2018 surveyed Hawaii tree canopy area within island/ecoregion combinations with mortality caused by insects and diseases. Tree canopy cover is based on data from a cooperative project between the Multi-Resolution Land Characteristics Consortium (Coulston and others 2012) and the Forest Service Geospatial Technology and Applications Center using the 2011 National Land Cover Database. See figure 1.2 for ecoregion identification. (Data source: U.S. Department of Agriculture Forest Service, Forest Health Protection)

LITERATURE CITED

Anselin, L. 1992. Spatial data analysis with GIS: an introduction to application in the social sciences. Tech. Rep. 92-10. Santa Barbara, CA: National Center for Geographic Information and Analysis. 53 p.

Barnes, I.; Fourie, A.; Wingfield, M.J. [and others]. 2018. New *Ceratocystis* species associated with rapid death of *Metrosideros polymorpha* in Hawaii. Persoonia-Molecular Phylogeny and Evolution of Fungi. 40(1): 154–181.

Berryman, E.; McMahan, A. 2019. Using tree canopy cover data to help estimate acres of damage. In: Potter, K.M.; Conkling, B.L., eds. Forest Health Monitoring: national status, trends, and analysis 2018. Gen. Tech. Rep. SRS-239. Asheville, NC: U.S. Department of Agriculture Forest Service, Southern Research Station: 125–141.

Brockerhoff, E.G.; Liebhold, A.M.; Jactel, H. 2006. The ecology of forest insect invasions and advances in their management. Canadian Journal of Forest Research. 36(2): 263–268.

Castello, J.D.; Leopold, D.J.; Smallidge, P.J. 1995. Pathogens, patterns, and processes in forest ecosystems. BioScience. 45(1): 16–24.

Cleland, D.T.; Freeouf, J.A.; Keys, J.E. [and others]. 2007. Ecological subregions: sections and subsections for the conterminous United States. Gen. Tech. Rep. WO-76D. Washington, DC: U.S. Department of Agriculture Forest Service. Map; Sloan, A.M., cartographer; presentation scale 1:3,500,000; colored. Also on CD-ROM as a GIS coverage in ArcINFO format or at http://data.fs.usda.gov/geodata/edw/datasets.php. [Date accessed: July 20, 2015].

Coulston, J.W.; Moisen, G.G.; Wilson, B.T. [and others]. 2012. Modeling percent tree canopy cover: a pilot study. Photogrammetric Engineering and Remote Sensing. 78(7): 715–727.

Edmonds, R.L.; Agee, J.K.; Gara, R.I. 2011. Forest health and protection. Long Grove, IL: Waveland Press, Inc. 667 p.

ESRI. 2015. ArcMap® 10.3. Redlands, CA: Environmental Systems Research Institute, Inc.

Forest Health Protection (FHP). 2016. Detection surveys. Fort Collins, CO: U.S. Department of Agriculture Forest Service, Forest Health Technology Enterprise Team. http://www.fs.fed.us/foresthealth/technology/detection_surveys.shtml. [Date accessed: July 23, 2016].

Forest Health Protection (FHP). 2019. Insect and Disease Detection Survey database (IDS). [Online database]. Fort Collins, CO: U.S. Department of Agriculture Forest Service, Forest Health Technology Enterprise Team. https://www.fs.fed.us/foresthealth/applied-sciences/mapping-reporting/gis-spatial-analysis/detection-surveys.shtml#idsdownloads. [Date accessed: July 17, 2019].

Getis, A.; Ord, J.K. 1992. The analysis of spatial association by use of distance statistics. Geographical Analysis. 24(3): 189–206.

Holdenrieder, O.; Pautasso, M.; Weisberg, P.J.; Lonsdale, D. 2004. Tree diseases and landscape processes: the challenge of landscape pathology. Trends in Ecology & Evolution. 19(8): 446–452.

Homer, C.G.; Dewitz, J.A.; Yang, L. [and others]. 2015. Completion of the 2011 National Land Cover Database for the conterminous United States: representing a decade of land cover change information. Photogrammetric Engineering and Remote Sensing. 81(5): 345–354.

Laffan, S.W. 2006. Assessing regional scale weed distributions, with an Australian example using *Nassella trichotoma*. Weed Research. 46(3): 194–206.

Liebhold, A.M.; McCullough, D.G.; Blackburn, L.M. [and others]. 2013. A highly aggregated geographical distribution of forest pest invasions in the USA. Diversity and Distributions. 19: 1208–1216.

Logan, J.A.; Regniere, J.; Powell, J.A. 2003. Assessing the impacts of global warming on forest pest dynamics. Frontiers in Ecology and the Envionment. 1: 130–137.

Lovett, G.M.; Weiss, M.; Liebhold, A.M. [and others]. 2016. Nonnative forest insects and pathogens in the United States: impacts and policy options. Ecological Applications. 26: 1437–1455.

Mack, R.N.; Simberloff, D.; Lonsdale, W.M. [and others]. 2000. Biotic invasions: causes, epidemiology, global consequences, and control. Ecological Applications. 10(3): 689–710.

Manion, P.D. 2003. Evolution of concepts in forest pathology. Phytopathology. 93: 1052–1055.

Parry, D.; Teale, S.A. 2011. Alien invasions: the effects of introduced species on forest structure and function. In: Castello, J.D.; Teale, S.A., eds. Forest health: an integrated perspective. New York: Cambridge University Press: 115–162.

Potter, K.M. 2012. Large-scale patterns of insect and disease activity in the conterminous United States and Alaska from the national Insect and Disease Detection Survey database, 2007 and 2008. In: Potter, K.M.; Conkling, B.L., eds. Forest Health Monitoring 2009 national technical report. Gen. Tech. Rep. SRS-167. Asheville, NC: U.S. Department of Agriculture Forest Service, Southern Research Station: 63–78.

Potter, K.M. 2013. Large-scale patterns of insect and disease activity in the conterminous United States and Alaska from the national Insect and Disease Detection Survey, 2009. In: Potter, K.M.; Conkling, B.L., eds. Forest Health Monitoring: national status, trends, and analysis 2010. Gen. Tech. Rep. SRS-176. Asheville, NC: U.S. Department of Agriculture Forest Service, Southern Research Station: 15–29.

Potter, K.M.; Escanferla, M.E.; Jetton, R.M.; Man, G. 2019a. Important insect and disease threats to United States tree species and geographic patterns of their potential impacts. Forests. 10(4): 304.

Potter, K.M.; Escanferla, M.E.; Jetton, RM. [and others]. 2019b. Prioritizing the conservation needs of United States tree species: evaluating vulnerability to forest insect and disease threats. Global Ecology and Conservation. 18: e00622.

Potter, K.M.; Koch, F.H. 2012. Large-scale patterns of insect and disease activity in the conterminous United States and Alaska, 2006. In: Potter, K.M.; Conkling, B.L., eds. Forest Health Monitoring 2008 national technical report. Gen. Tech. Rep. SRS-158. Asheville, NC: U.S. Department of Agriculture Forest Service, Southern Research Station: 63–72.

Potter, K.M.; Koch, F.H.; Oswalt, C.M.; Iannone, B.V. 2016. Data, data everywhere: detecting spatial patterns in fine-scale ecological information collected across a continent. Landscape Ecology. 31: 67–84.

Potter, K.M.; Paschke, J.L. 2013. Large-scale patterns of insect and disease activity in the conterminous United States and Alaska from the national Insect and Disease Detection Survey database, 2010. In: Potter, K.M.; Conkling, B.L., eds. Forest Health Monitoring: national status, trends, and analysis 2011. Gen. Tech. Rep. SRS-185. Asheville, NC: U.S. Department of Agriculture Forest Service, Southern Research Station: 15–28.

Potter, K.M.; Paschke, J.L. 2014. Large-scale patterns of insect and disease activity in the conterminous United States and Alaska from the national Insect and Disease Survey database, 2011. In: Potter, K.M.; Conkling, B.L., eds. Forest Health Monitoring: national status, trends, and analysis 2012. Gen. Tech. Rep. SRS-198. Asheville, NC: U.S. Department of Agriculture Forest Service, Southern Research Station: 19–34.

Potter, K.M.; Paschke, J.L. 2015a. Large-scale patterns of insect and disease activity in the conterminous United States and Alaska from the national Insect and Disease Survey, 2012. In: Potter, K.M.; Conkling, B.L., eds. Forest Health Monitoring: national status, trends, and analysis 2013. Gen. Tech. Rep. SRS-207. Asheville, NC: U.S. Department of Agriculture Forest Service, Southern Research Station: 19–36.

Potter, K.M.; Paschke, J.L. 2015b. Large-scale patterns of insect and disease activity in the conterminous United States, Alaska, and Hawaii from the national Insect and Disease Survey, 2013. In: Potter, K.M.; Conkling, B.L., eds. Forest Health Monitoring: national status, trends, and analysis 2014. Gen. Tech. Rep. SRS-209. Asheville, NC: U.S. Department of Agriculture Forest Service, Southern Research Station: 19–38.

Potter, K.M.; Paschke, J.L. 2016. Large-scale patterns of insect and disease activity in the conterminous United States and Alaska from the national Insect and Disease Survey, 2014. In: Potter, K.M.; Conkling, B.L., eds. Forest Health Monitoring: national status, trends, and analysis 2015. Gen. Tech. Rep. SRS-213. Asheville, NC: U.S. Department of Agriculture Forest Service, Southern Research Station: 21–40.

Potter, K.M.; Paschke, J.L. 2017. Large-scale patterns of insect and disease activity in the conterminous United States and Alaska from the national Insect and Disease Survey, 2015. In: Potter, K.M.; Conkling, B.L., eds. Forest Health Monitoring: national status, trends, and analysis 2016. Gen. Tech. Rep. SRS-222. Asheville, NC: U.S. Department of Agriculture Forest Service, Southern Research Station: 21–42.

Potter, K.M.; Paschke, J.L.; Zweifler, M. 2018. Large-scale patterns of insect and disease activity in the conterminous United States, Alaska, and Hawaii from the national Insect and Disease Survey, 2016. In: Potter, K.M.; Conkling, B.L., eds. Forest Health Monitoring: national status, trends, and analysis 2017. Gen. Tech. Rep. SRS-233. Asheville, NC: U.S. Department of Agriculture Forest Service, Southern Research Station: 23–44.

Potter, K.M.; Paschke, J.L.; Koch, F.H.; Zweifler, M. 2019. Large-scale patterns of insect and disease activity in the conterminous United States, Alaska, and Hawaii from the national Insect and Disease Survey, 2017. In: Potter, K.M.; Conkling, B.L., eds. Forest Health Monitoring: national status, trends, and analysis 2018. Gen. Tech. Rep. SRS-239. Asheville, NC: U.S. Department of Agriculture Forest Service, Southern Research Station: 21–49.

Reams, G.A.; Smith, W.D.; Hansen, M.H. [and others]. 2005. The Forest Inventory and Analysis sampling frame. In: Bechtold, W.A.; Patterson, P.L., eds. The enhanced Forest Inventory and Analysis program—national sampling design and estimation procedures. Asheville, NC: U.S. Department of Agriculture Forest Service, Southern Research Station: 11–26.

Shima, T.; Sugimoto, S.; Okutomi, M. 2010. Comparison of image alignment on hexagonal and square lattices. In: 2010 IEEE international conference on image processing. [Place of publication unknown]: Institute of Electrical and Electronics Engineers, Inc.: 141–144. DOI: 10.1109/icip.2010.5654351.

Smith, W.B.; Miles, P.D.; Perry, C.H.; Pugh, S.A. 2009. Forest resources of the United States, 2007. Gen. Tech. Rep. WO-78. Washington, DC: U.S. Department of Agriculture Forest Service. 336 p.

Spencer, P.; Nowacki, G.; Fleming, M. [and others]. 2002. Home is where the habitat is: an ecosystem foundation for wildlife distribution and behavior. Arctic Research of the United States. 16: 6–17.

Teale, S.A.; Castello, J.D. 2011. Regulators and terminators: the importance of biotic factors to a healthy forest. In: Castello, J.D.; Teale, S.A., eds. Forest health: an integrated perspective. New York: Cambridge University Press: 81–114.

Tobin, P.C. 2015. Ecological consequences of pathogen and insect invasions. Current Forestry Reports. 1: 25–32.

University of Hawai‘i, College of Tropical Agriculture and Human Resources. 2019. Rapid ‘ōhi‘a death/*Ceratocystis* wilt of ‘ōhi‘a. http://rapidohiadeath.org. [Date accessed: August 9, 2019].

U.S. Department of Agriculture (USDA) Forest Service. 2008. National forest type data development. http://svinetfc4.fs.fed.us/rastergateway/forest_type/. [Date accessed: May 13, 2008].

White, D.; Kimerling, A.J.; Overton, W.S. 1992. Cartographic and geometric components of a global sampling design for environmental monitoring. Cartography and Geographic Information Systems. 19(1): 5–22.

Zhang, L.; Rubin, B.D.; Manion, P.D. 2011. Mortality: the essence of a healthy forest. In: Castello, J.D.; Teale, S.A., eds. Forest health: an integrated perspective. New York: Cambridge University Press: 17–49.